Synthesis of fault geometry, seismicity, and deep structural fabric to constrain Community Fault (CFM) and Rheology (CRM) Models

Principal Investigators: Deborah Kilb (UCSD - Scripps Institution of Oceanography) and Vera Schulte-Pelkum (University of Colorado Boulder)

Abstract

We combine newly available southern California data sets to provide constraints for refinement of the SCEC Community Fault Model (CFM) as well as development of the Community Rheology Model (CRM). We compare CFM 5.3, contrasts in rock fabric imaged by receiver functions, and microseismicity in the GrowClust and QTM catalogs. Our work leverages recent receiver function results using azimuthal harmonic arrivals to image the depth, amplitude, and strike of conversions from contrasts in dipping foliation and dipping contrasts between isotropic bodies, an approach particularly well suited to mapping shear zones, dipping faults, and tectonic boundaries. We highlight general parallelism of receiver function-derived crustal fabric strikes with strikes of nearby faults in the CFM and find multiple instances of alignment of receiver function-derived strikes with planar features delineated in relocated seismicity. Below the seismogenic zone, we find lower crustal distributed fabric in the southern Sierra Nevada paralleling exhumed ductile fabric aligning with the reactivated Kern Canyon Fault. We also find near-fault structure imaged by data from dense station deployments along the San Jacinto fault and the San Andreas Fault near Parkfield showing deep pervasive fault-parallel fabric, fine structure of the Ridgecrest and Coso areas with orthogonal features in seismicity and receiver function imaging, and fabric contrasts imaged at the boundaries of crustal conductors from magnetotellurics. In most of southern California, deep distributed fabric aligns with past tectonics. Rather than defining individual shear zone geometries, we favor an approach that defines anisotropy of viscosity in lithospheric blocks.

Science Highlights

CXM

SDOT

Seismology

Exemplary Figure

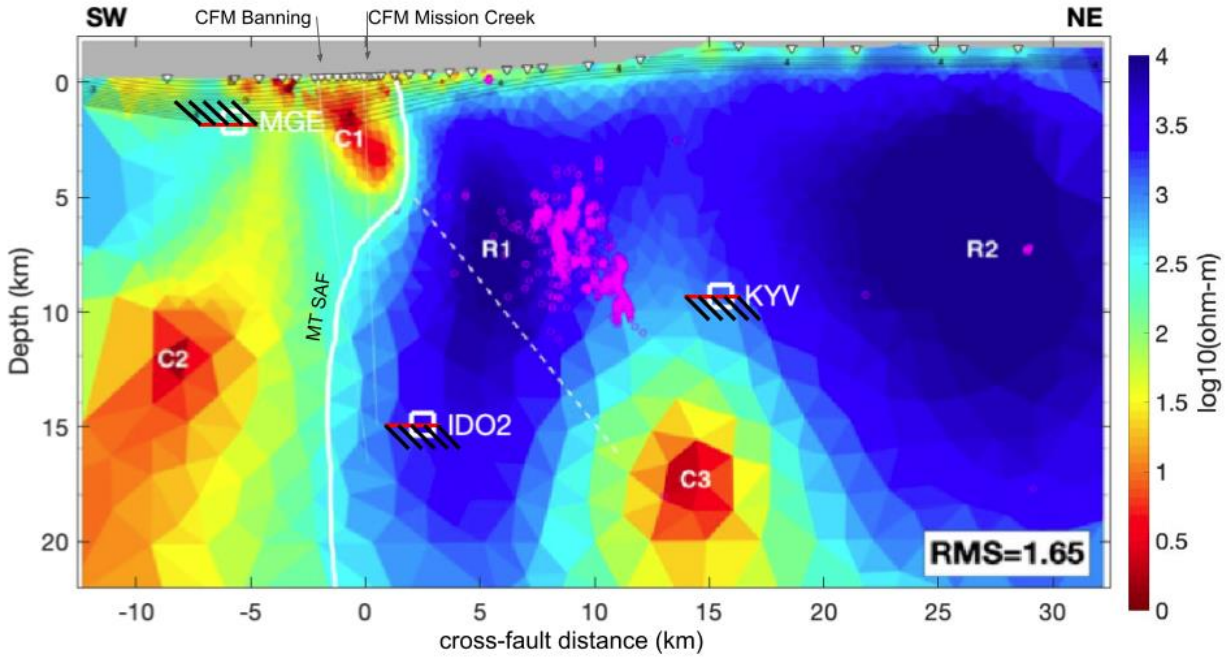

Figure 2: Cross section perpendicular to the SSAF north of the Salton Sea. QTM relocated seismicity (pink), inverted resistivity from MT (background color), inferred SAF (thick white), and CFM surface faults (thin white) from Share et al. (2023); RF harmonic arrivals (white squares) with fabric dip sense (black bars) above/below converting contrast (red).

SCEC Science Priorities

1. **3.b** Constrain the active geometry and rheology of the ductile roots of fault zones. (CXM , SDOT, FARM, Geology)
2. **3.a** Refine the geometry of active faults across the full range of seismogenic depths, including structures that link and transfer deformation between faults. (CXM, Seismology, Geodesy, Geology, SAFS)

3. **1.b** Determine the spatial scales at which tectonic block models (compared to continuum models) provide descriptions of fault-system deformation that are useful for earthquake forecasting. (SDOT, Geodesy, EFP, CXM)

Intellectual Merit

We use newly available data sets to provide constraints for **refinement of the SCEC Community Fault (CFM)** as well as **development of the Community Rheology (CRM) models**, both in accordance with SCEC5 research goals. This suite of independent data include the CFM 5.3 (*Maechling et al.*, 2020; *Nicholson et al.*, 2020; *Plesch et al.*, 2020), receiver function (RF) imaging of faults and intracrustal tectonic structural grain (*Schulte-Pelkum et al.*, 2020b), and refined earthquake catalogs that include a template-based catalog (*Ross et al.*, 2019) and updates to the SCSN catalog (*Hauksson et al.*, 2012) including the GrowClust version (*Trugman and Shearer*, 2017). The synthesis of the CFM and catalog products with our

RF deep crustal fabric imaging is an original approach that supports improvements to CFM geometries, particularly at depth, and provides constraints for shear zones and block rheology for the CRM.

Broader Impacts

A strength of this work is the cross-disciplinary aspect of the study, that includes data and resources from seismicity catalogs, 3D receiver function imaging, and 3D geologic fault models. Regular interaction between researchers within these sub-disciplines leads to cross-fertilization between the different CXMs, which in turn increases their value beyond the SCEC community. Discussions at the 2021 SCEC annual meeting with geologists, CFM researchers, geodynamicists, and seismologists have already opened new research avenues. Improvements to the CXMs benefit broader society through e.g., improved hazard estimates. Results were presented at the SCEC annual meeting, at AGU Fall meetings, and as part of a lectures in undergraduate classes.

Project Publications

Schulte-Pelkum, V., & Kilb, D. (2021, 08). Synthesis of fault geometry, seismicity, and deep structural fabric to constrain Community Fault (CFM) and Rheology (CRM) Models. Poster Presentation at 2021 SCEC Annual Meeting.

Kilb, D. L., Schulte-Pelkum, V., Becker, T. W., Behr, W. M., & Miller, M. S. (2021, December). Past and Present Deformation along the San Andreas from Microseismicity, Geodesy, and Seismological Constraints. In AGU Fall Meeting 2021. AGU.

Kilb, D.L. and V. Schulte-Pelkum (2022). Deep crustal deformation from the Central San Andreas fault through the Sierra Nevada from seismicity and anisotropic receiver functions, American Geophysical Union, T44A-03, Chicago, Illinois.

Schulte-Pelkum V., D. L. Kilb, W. J. Shinevar (2023). Lithospheric Removal and Moho Modification in Active Orogens: Examples from the Sierra Nevada and Tibetan Plateau, American Geophysical Union, T43E-0305, San Francisco, California.

FINAL TECHNICAL REPORT

Synthesis of fault geometry, seismicity, and deep structural fabric to constrain Community Fault (CFM) and Rheology (CRM) Models

Principal Investigators: Deborah Kilb (UCSD - Scripps Institution of Oceanography) and Vera Schulte-Pelkum (University of Colorado Boulder)

PROJECT PURPOSE. This project uses a triad of data sets (CFM 5.3 fault structure, receiver function (RF) azimuthal harmonic arrivals, and 3D seismicity distributions) to achieve improved understanding of fault and shear zone structures. The overall goal is to derive constraints for refinement of the Southern California Earthquake Center (SCEC) Community Fault Model (CFM) and the development of the Community Rheology Model (CRM).

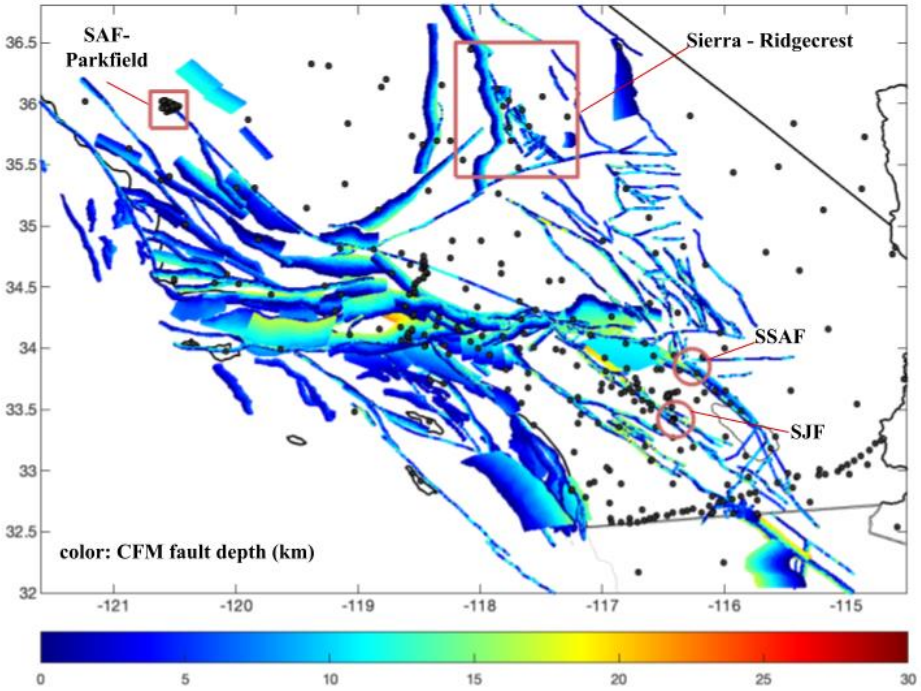

Fig. 1: Study area: CFM5.3 fault depths, RF station locations (black dots), Figs. 2-5 locations.

INTRODUCTION. Deformation in southern California is expressed in active faults (Fig. 1), mapped in 3D by the SCEC Community Fault Model (CFM, currently version 5.3; Maechling et al., 2020; Nicholson et al., 2020; Plesch et al., 2020a); microseismicity as catalogued by SCSN as well as several other methods (Hauksson et al., 2012, Ross et al., 2019); and crustal rock fabric as imaged by methods that target seismic anisotropy, e.g., local event shear wave splitting (most recently, Li & Peng, 2017) and receiver function analysis (e.g., Porter et al., 2011; Schulte-Pelkum et al., 2020b). On a lithospheric scale, Schulte-Pelkum et al. (2021) compiled deformation markers from seismic anisotropy, geodesy, and focal mechanisms to infer a significant influence on inherited fabric from prior subduction, extension, and block rotation on present-day behavior. This project focuses on constraints from the seismogenic crust as provided by the CFM and seismicity catalogs, with extension to below seismogenic depths in the crust as provided by receiver function-based imaging of rock fabric. The latter effort will inform practices for the CRM under development.

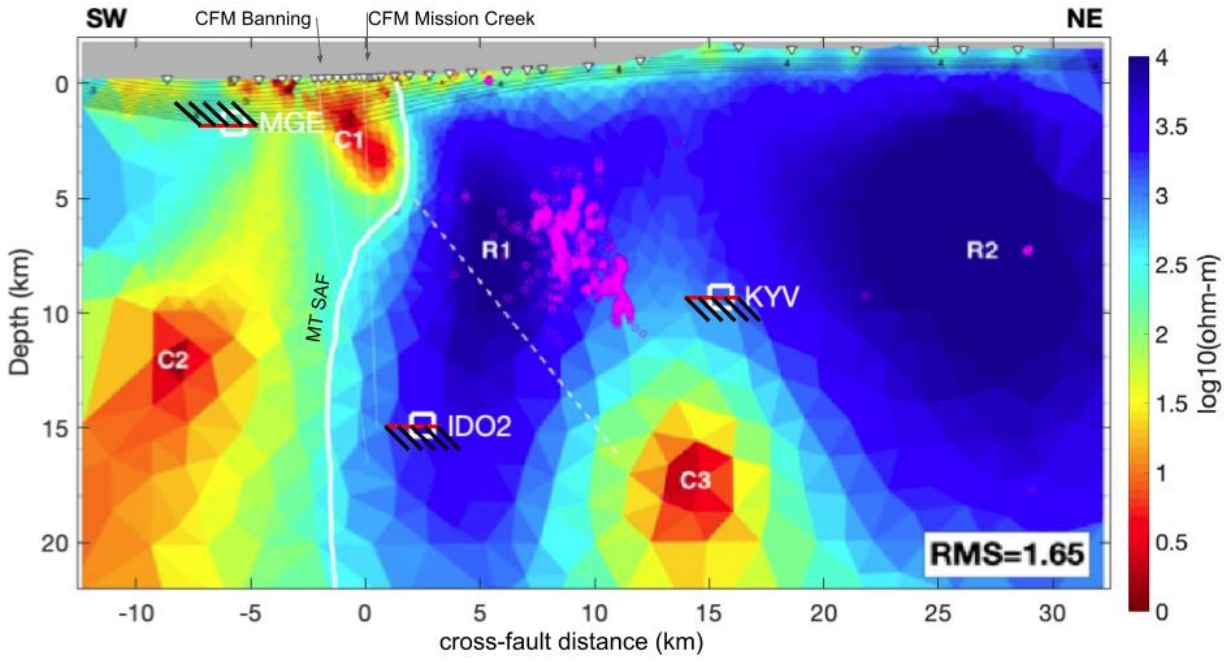

Fig. 2: Cross section perpendicular to the southern San Andreas fault (SSAF) north of the Salton Sea (Fig. 1). QTM relocated seismicity (pink), inverted resistivity from MT (background color), inferred SAF (thick white), and CFM surface faults (thin white), modified from Share et al. (2023); RF harmonic arrivals (white squares, strikes parallel SAF) with fabric dip sense (black bars) above/below converting contrast (red).

DATA. This work relies on three primary data sets. (1) 3-D CFM 5.3 fault geometry (Hearn et al., 2020; Hughes et al., 2020). (2) 3-D tectonic grain as imaged by receiver functions (RF) (Schulte-Pelkum, Ross, et al., 2020); and (3) 3-D Seismicity: 1981-2017 SCSN catalog (Hauksson et al., 2012), including locations from the GrowClust algorithm (Trugman and Shearer, 2017), supplemented by a denser 10-year template catalog (Ross et al., 2019).

METHOD. We conduct a 3-D comparison of the three different multi-dimensional data sets. We use the CFM5.3 fault orientations, structures mapped by the relocated seismicity, strikes of fabric at a contrast mapped by harmonic RFs, depth of the harmonic RF conversion, and dip direction as inferred from the RF arrival phase.

RESULTS. In this final report, we present results from four regions within southern California (Fig. 1): southern SAF (SSAF) near the Banning/Mission Creek fault convergence, the SAF near Parkfield, the San Jacinto Fault (SJF) zone, and the southern Sierra Nevada to Ridgecrest area.

SSAF near the Salton Sea. Two surface strands of the SAF (Banning and Mission Creek faults) merge into a single surface strand north of the Salton Sea (Fig. 1). A recent magnetotelluric profile and inversion (Share et al., 2023) inferred NE-dipping near-surface structures (also e.g. Lin et al., 2007; Fuis et al., 2017), a subvertical deep SSAF, and a conductive structure NE of the inferred SSAF that appears as an extension of NE-dipping microseismicity. RF harmonic arrivals indicating fabric contrasts appear near the edges of conductive structures (Fig. 2; stations IDO, KYV) or basement boundary (MGF), with fabric that shows SSAF-parallel strikes and polarities that are consistent with NE dipping foliation.

San Jacinto Fault Zone. A dense broadband station deployment (Vernon & Ben-Zion, 2010) crosses the central fault strand and extends to the SW (Fig. 3). CFM faults are subvertical. Seismicity suggests lineations dipping steeply to the SW as well as NE. RF-imaged fabric is consistent with pervasive NE dips, with fast plane strikes that are fault-parallel but show a slight rotation atop the central fault strand, possibly related to a damage zone.

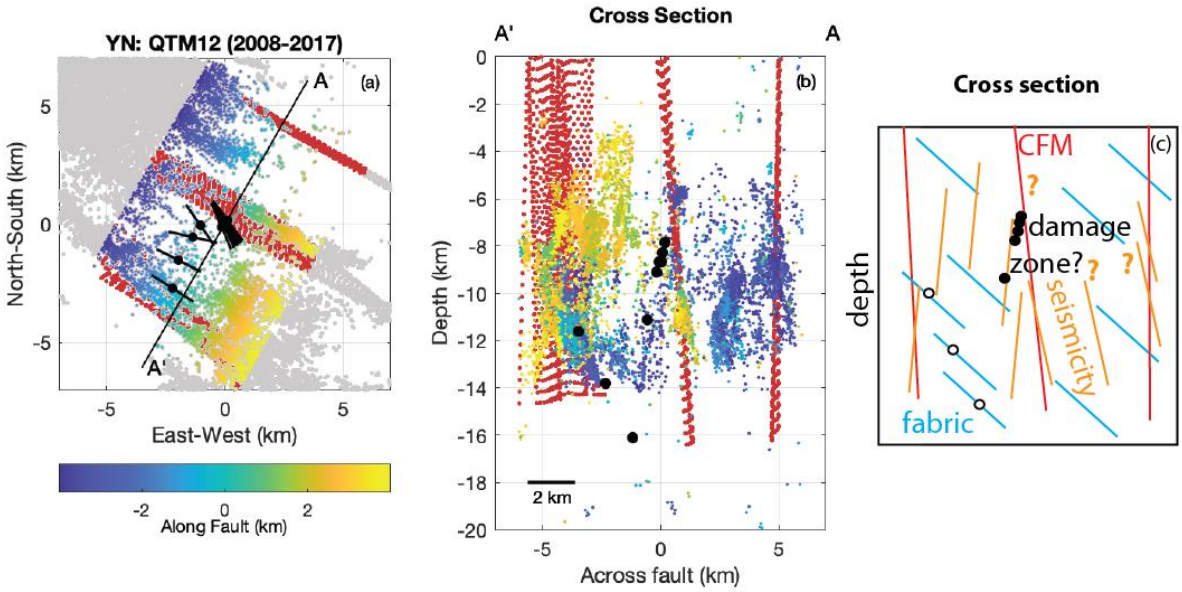

Fig. 3: San Jacinto Fault zone near the trifurcation region (Clark fault, Coyote Creek fault, and Buckridge fault) centered at (-116.38,33.43). Data include CFM5.3 faults (red), QTM seismicity (points, colored by along fault location) and RF azimuths (black bars) and RF depths (black circles) from stations in the YN network deployment. (a) The general strike of the CFM faults is N45E. (b) Depth cross section shows the seismicity in this region is complex, primarily mapping steeply dipping structures that have slightly different fault strikes and dips. (c) Schematic interpretation of these results as a coexistence of a fault fabric dipping to the north east (cyan, from RF) interacting with active steeply dipping fault structures (orange from seismicity; red from CFM) with near-fault harmonic RF conversions possibly outlining a damage zone.

San Andreas Fault near Parkfield. The maximum northern extent of data along the SAF for the QTM catalog and CFM are latitudes 37° and 36°, respectively, placing Parkfield at the northern extent of both datasets. Here, we use a dense broadband network (PASO; Thurber et al., 2003, 2004), borehole stations of the PB network, and the GrowClust catalog. Strikes of RF-imaged fast planes (Fig. 4) are consistently parallel with the NE-striking SAF surface trace. The depth distribution of the largest first azimuthal harmonic conversion at each station deepens away from a vertical fault as mapped by GrowClust seismicity (Fig. 4). Interestingly, polarities of the first harmonic maximum arrival for stations on both sides of the fault are positive to the NE, consistent with a NE-dipping fabric. Receiver function azimuthal first harmonic conversion amplitudes are noticeably larger on the NE side of the SAF compared to the SW side. A possible interpretation of these observations is inherited Farallon fabric with intermediate NE dip that is reactivated as an incipient SAF with dipping geometry (Fig. 4, green line) which progressively steepens to its present

day subvertical geometry (Fig. 4, red) as proposed for other major faults in this area (Mason et al., 2017; Dorsey et al., 2012).

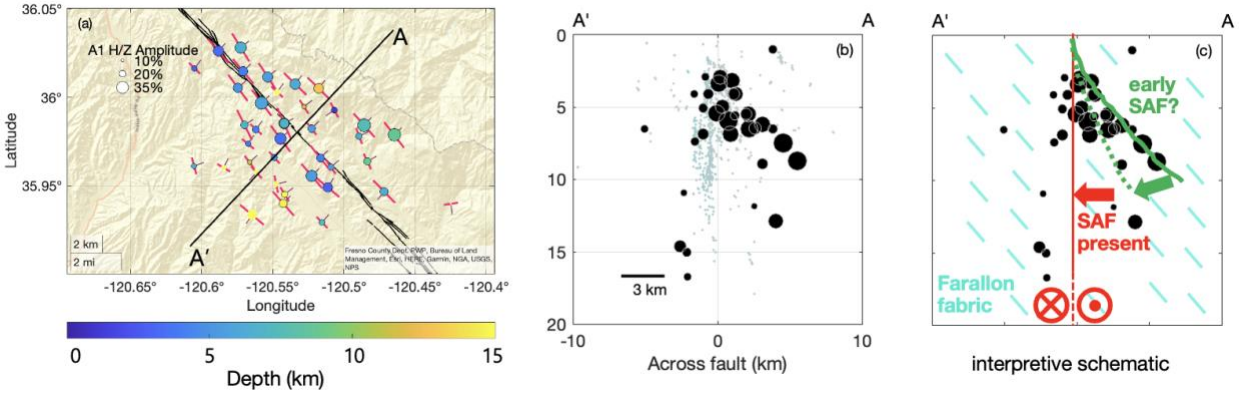

Figure 4: (a) Map view of the San Andreas Fault (SAF) near Parkfield with stations (circles, scaled by amplitude of the largest first azimuthal harmonic arrival, colored by depth of the converter), receiver function-derived subsurface foliation strikes (red bars) and foliation dip azimuth (brown tickmarks); faults from the USGS database in black. (b) Depth cross section with seismicity (grey) from the GrowClust catalog (Trugman and Shearer, 2017); receiver function conversion depths as black circles, scaled by amplitude as in a. (c) Conceptual sketch: Preexisting fabric (cyan) may be enhanced by an incipient SAF (curved green line) that proceeds to straighten (dotted green line) to its present vertical geometry (red) (Mason et al., 2017; Dorsey et al., 2012).

Ridgecrest, Coso, Sierra Nevada. Studies of the July 2019 Ridgecrest M6.4 and M7.1 earthquakes and aftershocks found a prevalence of perpendicular conjugate fault structures within the region (e.g., Ross et al., 2019; Plesch et al., 2020b). RF fabric strikes are consistent with these findings, and our results show orthogonal features in both seismicity and receiver function imaging (see Fig. 2). In the Sierra Nevada region, the Kern Canyon CFM5.3 fault model extends to a depth of 15 km, and the nearby seismicity extends to depths of 20 km and 25 km for GrowCluster and QTM, respectively. The RF results, however, allow us to obtain information about the fault fabric below the seismogenic zone and past Moho depths. We find a shear layer extending from the Moho down to an uppermost mantle interface ~20 km below the Moho with geometry consistent of westward removal of a lithospheric root as proposed previously (e.g. Saleeby et al., 2003; Zandt et al., 2004; Fig. 5).

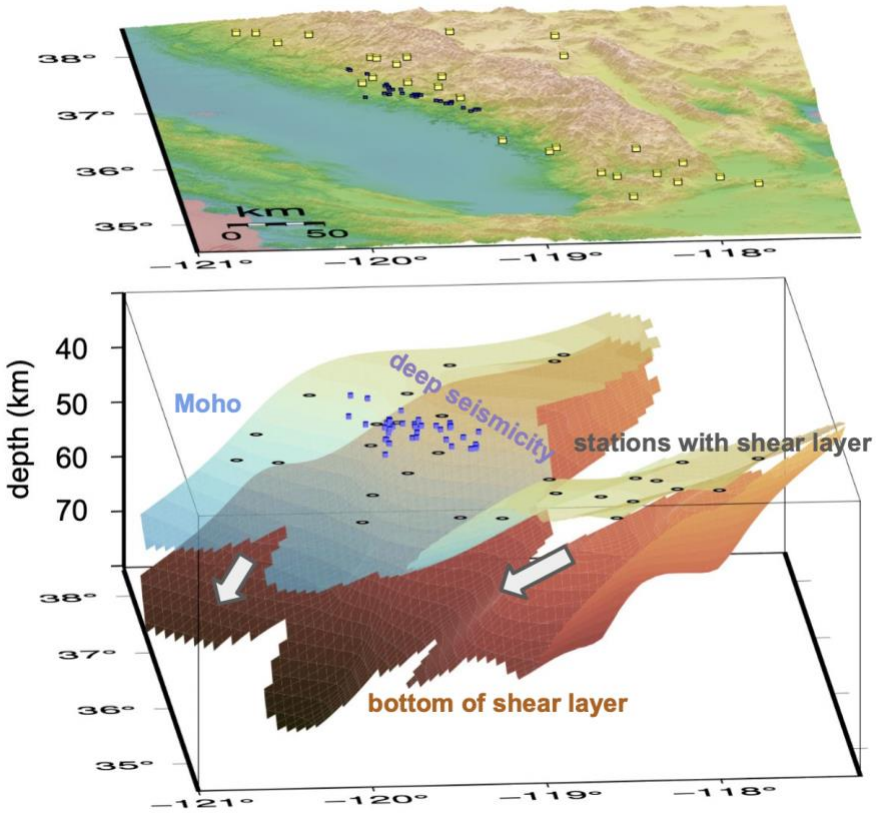

Fig. 5. Stations in the Sierra Nevada (yellow boxes) show Moho (blue interface, fitted to grey circles) and sub-Moho (red interface) arrivals from boundaries of a sub-Moho shear layer with geometry consistent with westward foundering of lithosphere (white arrows) that has concluded in the south and is ongoing in the central Sierra as indicated by seismicity with depth greater than 40 km (blue boxes).

SUMMARY AND CONCLUSIONS

This work leverages recent RF results using azimuthal harmonic arrivals to image the depth, amplitude, and strike of conversions from contrasts in dipping foliation and dipping contrasts between isotropic bodies, an approach particularly well suited to mapping shear zones, dipping faults, and tectonic boundaries (Schulte-Pelkum et al., 2014a,b, 2020a,b). We compare these RF strike orientations and depths with those from the SCEC CFM5.3 and relocated seismicity catalogs (QTM and GrowClust). We find general parallelism of RF-derived crustal fabric strikes with strikes of nearby faults in the CFM5.3 and also find multiple instances of alignment of RF-derived strikes with planar features delineated in the relocated seismicity. Comparison with a recent MT results along the SSAF suggests that contrasts in imaged rock fabric may relate to contrasts in resistivity. Below the seismogenic zone, the RF data show deep crustal distributed fabric paralleling surface fault orientations. We also find near-fault structure imaged by data from dense station deployments along the SJF and the SAF near Parkfield showing damage zones resulting from fault-parallel inherited fabric with present-day deformation, as well as fine structure of the Ridgecrest and Coso areas with orthogonal features in seismicity and RF imaging. Given the pervasive fabric orientations, we favor a CRM approach that defines anisotropy of viscosity in lithospheric blocks rather than detailing individual shear zone geometries.

References Cited

Dorsey, R. J., G. J. Axen, T. C. Peryam, and M. E. Kairouz, Initiation of the Southern Elsinore Fault at similar to 1.2 Ma: Evidence from the Fish Creek-Vallecito Basin, southern California, Tectonophys., 31, doi:10.1029/2011TC003009, 2012.

Fuis, G. S., Bauer, K., Goldman, M. R., Ryberg, T., Langenheim, V. E., Scheirer, D. S., & Aagaard, B. (2017). Subsurface geometry of the San Andreas Fault in Southern California: Results from the Salton Seismic Imaging Project (SSIP) and strong ground motion expectations. *Bulletin of the Seismological Society of America*, 107, 1642– 1662.

Hauksson, E., W. Yang, and P. M. Shearer, Waveform Relocated Earthquake Catalog for Southern California (1981 to June 2011), *Bulletin of the Seismological Society of America*, *102*(5), 2239–2244, doi:10.1785/0120120010, 2012.

Hearn, L., S. Marshall, and L. Montesi, Highlights of SCEC Community Modeling Efforts and a Vision for Community Models in the Next Earthquake Center, 2020.

Hughes, A., R. Bell, Z. Mildon, D. Rood, A. Whittaker, T. Rockwell, Y. Levy, D. DeVecchio, S. Marshall, and C. Nicholson, Three-dimensional structure, ground rupture hazards, and static stress models for complex nonplanar thrust faults in the ventura basin, southern california, *Journal of Geophysical Research: Solid Earth*, *125*(7), e2020JB019,539, 2020.

Li, Z., and Z. Peng, Stress-and structure-induced anisotropy in southern California from two decades of shear wave splitting measurements. *Geophysical Research Letters*, *44*(19), 9607-9614, 2017.

Lin, G., P. M. Shearer, and E. Hauksson, Applying a three-dimensional velocity model, waveform cross correlation, and cluster analysis to locate southern California seismicity from 1981 to 2005, *Journal of Geophysical Research - Solid Earth*, *112*(B12), doi:10.1029/ 2007JB004986, 2007.

Maechling, P., M. Su, E. Hearn, S. Marshall, A. Plesch, S. J.H., O. M.E., M. L.G., P. E., H. T.T., and B. Y., Developing Web-based Visualization and Query Tools for the SCEC CVM, CFM, GFM, and CTM Community Models, *Poster Presentation at 2020 SCEC Annual Meeting*, 2020.

Mason, C. C., J. A. Spotila, G. Axen, R. J. Dorsey, A. Luther, and D. F. Stockli, Two-Phase Exhumation of the Santa Rosa Mountains: Low- and High-Angle Normal Faulting During Initiation and Evolution of the Southern San Andreas Fault System, Tectonophys., 36, 2863–2881, doi:10.1002/2017TC004498, 2017.

Nicholson, C., A. Plesch, C. Sorlien, J. H. Shaw, and E. Hauksson, Updates, Evaluation and Improvements to the Community Fault Model (CFM version 5.3), *Poster Presentation at 2020 SCEC Annual Meeting*, 2020.

Perrin, C., Waldhauser, F., Choi, E., & Scholz, C. H. (2019). Persistent fine-scale fault structure and rupture development: A new twist in the Parkfield, California, story. *Earth and Planetary Science Letters*, *521*, 128-138.

Plesch, A., S. Marshall, C. Nicholson, P. J. Maechling, and M. Sue, The Community Fault Model version 5.3 and new web-based tools., *Poster Presentation at 2020 SCEC Annual Meeting*, 2020a.

Plesch, A., J. H. Shaw, Z. E. Ross, and E. Hauksson, Detailed 3D Fault Representations for the 2019 Ridgecrest, California, Earthquake Sequence, *Bulletin of the Seismological Society of America*, *110*(4), 1818–1831, 2020b.

Porter, R., Zandt, G., & McQuarrie, N. Pervasive lower-crustal seismic anisotropy in Southern California: Evidence for underplated schists and active tectonics. *Lithosphere*, 3, 201–220. https://doi.org/10.1130/L126.1, 2011.

Ross, Z. E., D. T. Trugman, E. Hauksson, and P. M. Shearer, Searching for hidden earthquakes in Southern California, *Science*, *364*(6442), 767+, doi:10.1126/science.aaw6888, 2019.

Ross, Z. E., Idini, B., Jia, Z., Stephenson, O. L., Zhong, M., Wang, X., ... & Jung, J. (2019). Hierarchical interlocked orthogonal faulting in the 2019 Ridgecrest earthquake sequence. *Science*, *366*(6463), 346-351.

Saleeby, J., M. Ducea, and D. Clemens-Knott, Production and loss of high-density batholithic root, southern Sierra Nevada, California (2003), Tectonics, 22(6), 1064, doi:10.1029/ 2002TC001374.

Schulte-Pelkum, V., and K. H. Mahan, A method for mapping crustal deformation and anisotropy with receiver functions and first results from USArray, *Earth Planet. Sci. Lett.*, *402*(SI), 221–233, doi:10.1016/j.epsl.2014.01.050, 2014a.

Schulte-Pelkum, V., and K. H. Mahan, Imaging Faults and Shear Zones Using Receiver Functions, *Pure Appl. Geophys.*, *171*, 2967–2991, doi:10.1007/s00024-014-0853-4, 2014b.

Schulte-Pelkum, V., J. S. Caine, J. V. J. III, and T. W. B. Becker, Imaging the tectonic grain of the Northern Cordillera orogen using Transportable Array receiver functions, *Seismological Research Letters*, *91*(6), 3086–3105, doi:doi:10.1785/0220200182, 2020a.

Schulte-Pelkum, V., Z. Ross, K. Mueller, and Y. Ben-Zion, Tectonic inheritance with dipping faults and deformation fabric in the brittle and ductile southern California crust, *J. Geophys. Res.*, *125*(8), e2020JB019,525, doi:10.1029/2020JB019525, 2020b.

Schulte-Pelkum, V., Becker, T. W., Behr, W. M., & Miller, M. S. Tectonic inheritance during plate boundary evolution in southern California constrained from seismic anisotropy. *Geochemistry, Geophysics, Geosystems*, 22, e2021GC010099. https://doi. org/10.1029/2021GC010099, 2021.

Share, P. E., Peacock, J. R., Constable, S., Vernon, F. L., & Wang, S. (2023). Structural properties of the Southern San Andreas fault zone in northern Coachella Valley from magnetotelluric imaging. *Geophysical Journal International*, *232*(1), 694-704, 2023.

Thurber, C., S. Roecker, K. Roberts, M. Gold, L. Powell, and K. Rittger, Earthquake locations and three-dimensional fault zone structure along the creeping section of the San Andreas Fault near Parkfield, CA: preparing for SAFOD, *Geophys. Res. Lett.*, *30*, doi:doi:10.1029/2002GL016004, 2003.

Thurber, C., S. Roecker, H. Zhang, S. Baher, and W. Ellsworth, Fine-scale structure of the San Andreas fault and location of the SAFOD target earthquakes, *Geophys. Res. Lett.*, *31*, L12S02, doi:doi:10.1029/2003GL019398, 2004.

Trugman, D. T., & Shearer, P. M. GrowClust: A hierarchical clustering algorithm for relative earthquake relocation, with application to the Spanish Springs and Sheldon, Nevada, earthquake sequences. *Seismological Research Letters*, 379-391, 2017.

Vernon, F. & Yehuda Ben-Zion. San Jacinto Fault Zone Experiment. International Federation of Digital Seismograph Networks. https://doi.org/10.7914/SN/YN_2010, 2010.

Zandt, G., H. Gilbert, T. Owens, M. Ducea, J. Saleeby, C. Jones (2004), Active foundering of a continental arc root beneath the southern Sierra Nevada in California, Nature, 431, 41-46.